Impedance Behaviour of a Microporous PMMA-Film 'Coated Constant Phase Element' based Chemical Sensor

Karabi Biswas*, Litty Thomas+, Sourabh Chowdhury+, Basudam Adhikari!, and Siddhartha Sen+

*Department of Instrumentation & Electronics Engineering, Jadavpur University, Kolkata-700 098, India

+ Department of Electrical Engineering, Indian Institute of Technology, Kharagpur-721302, India

! Material Science Center, Indian Institute of Technology, Kharagpur-721302, India

E-mail: kbiswas@iee.jusl.ac.in

Abstract-In this work, it has been attempted to characterize a new type of impedance sensor called constant phase element (CPE) sensor; which has microporous PMMA-film coating on the electrode surface. It has been shown that the 'constant phase angle (CPA)' behaviour is primarily due to the porous structure of the electrode surface. And the phase angle at the output of the sensor changes with thickness variation of the PMMA coating and ionic property of the medium in which the sensor is dipped in. The sensor has been used for chemical sensing. A phase angle detector circuit gives the output in voltage with the change in the phase angle. The complex impedance plots of the probes has also been discussed. The important fact is that the constructed CPE gives rise to a fractional order system.

Key word: Chemical sensor, constant phase element, fractional order system, phase detector circuit.

I. Introduction

Chemical and biochemical sensors have emerged as an effective technique for quantitative and qualitative analysis in chemical diagnosis, environmental monitoring and food and process control [1], [2], [3]. As a result, there is a need for a low cost, reliable, sensitive and fast sensor [4]. In this work, a 'constant phase element (CPE)' sensor has been used for this purpose. It is a new type of impedance sensor, where the phase angle remains constant

(ideally for all the frequencies) and its impedance is represented by [5], [6], [7]

$$Z_{CPE} = Qs^{-\alpha}. \tag{1}$$

The coefficient Q and the fractional exponent α are the parameters of the CPE and s is the Laplace operator. This implies that for an ideal capacitance the phase angle is $-90°$, for an resistance it is $0°$ and for an CPE it can be any value between $0°$ to $-90°$.

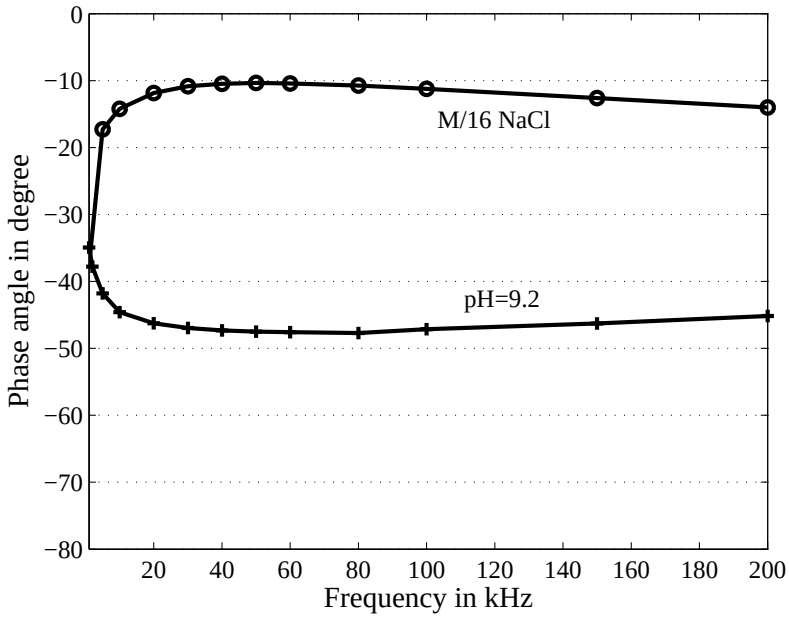

Figure 1. The CPA in the aqueous solution of pH=9.2 and in 1/16 molar NaCl solution.

The authors have reported the fabrication of a CPE by providing a thin coating of PMMA-film on the electrode surface of a capacitive type probe [8]. The probe gives a 'constant phase angle (CPA)' (Figure 1) when dipped in a polarizable medium as shown in Figure 2. The measurement has been performed with a precision LCR meter (HP 4284A) in Z and θ mode at the frequency range of 1 kHz to 1 MHz.

The constant phase angle behaviour of certain devices has been noted by many researchers working in the filed of elctrochemistry, power line transmission, communication, etc. [5], [9], [10], [11], [12], [13]. Researchers have also noted the potential of a CPE - as it is

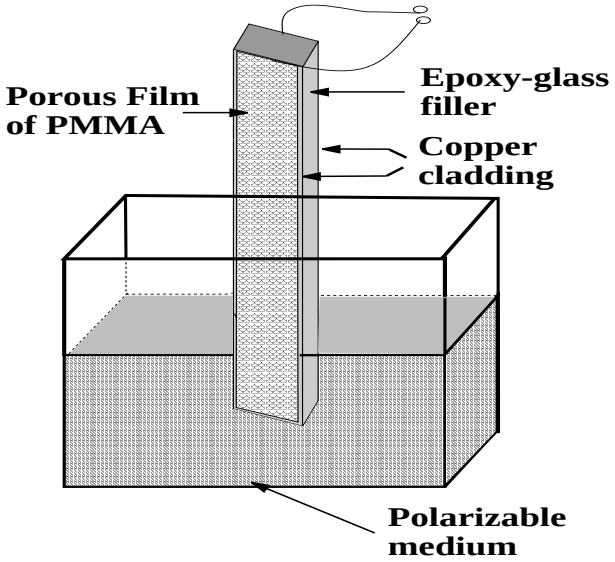

Figure 2. Construction of the CPE with microporous-PMMA-film coated electrode.

characterized as a fractional order system which is useful in many engineering applications [14], [15], [16], [17], [18], [19], [20].

In previous works, realization of a CPE and its use in two different engineering applications [8], [21] have been reported by the authors. In the present paper, further studies on the generation of the CPE behaviour of the PMMA coated probe has been reported. In this work, it has been revealed that the CPA behaviour is primarily due to the porosity of PMMA coating on the electrode surface. The paper discusses the porous structure of the PMMA film, the variation of CPA behaviour on different pore sizes and the impedance behaviour in different ionic media. The complex impedance plots in different ionic media show that the different boundary conditions of diffusion can be observed by the constructed CPE.

The performance of the the sensor for chemical changes has been studied. The response of the sensor to different molar concentration of NaCl, KCl, NH_4OH and Urea are reported in the paper.

The paper is organised as: in section-2, development of the porous structure of the PMMA film on the copper electrode is described. CPA behaviour of the porous electrode is discussed in section-3. Section-4 gives the complex impedance plots of the sensor in different

polarizable media. In section-5, the performance of the CPE as chemical sensor has been reported. Section-6 discusses the results and section-7 gives conclusion.

II. Developing porous structure of the PMMA film

The thin layer of PMMA coating is provided on the copper electrodes by inserting the probe in PMMA-chloroform solution [8]. The probe is made from a double layer copper cladded PCB, generally used for discrete circuit fabrication. To monitor the thickness of

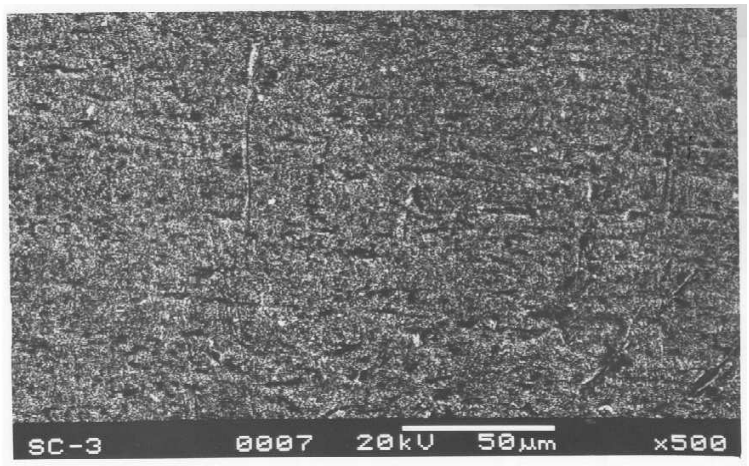

Figure 3. Bare surface of the electrode before coating.

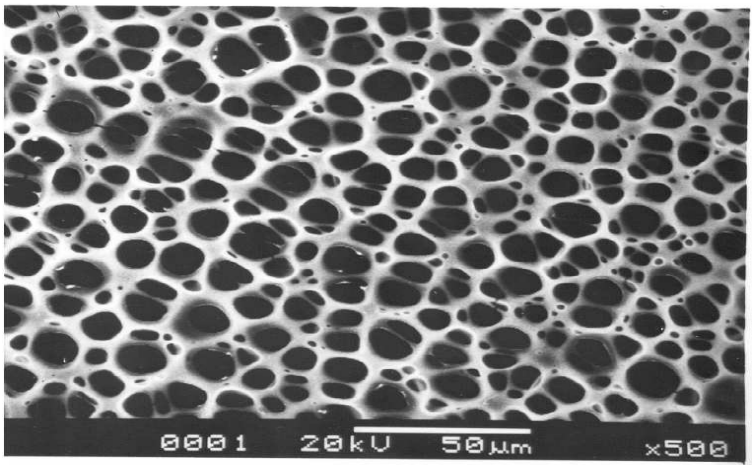

Figure 4. Porous surface of the electrode after coating: coating thickness is 5 μm. Diameter of the pore is about 10 μm.

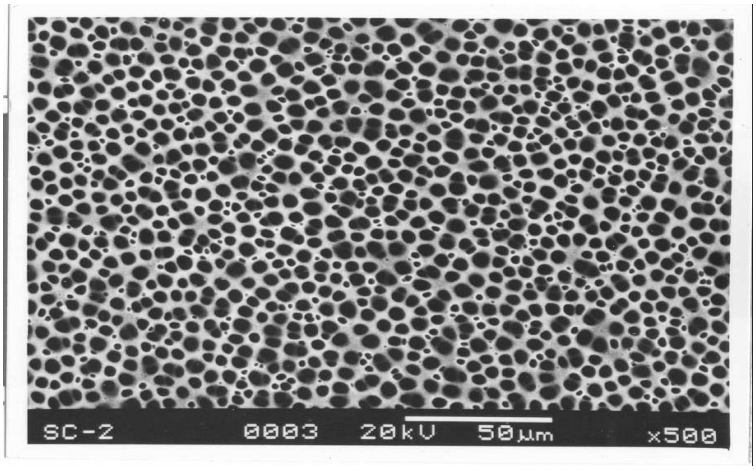

Figure 5. Porous surface of the electrode after coating: coating thickness is 12 μm. Diameter of the pore is about 5 μm.

the coating, the probe thickness is measured by an industrial grade dial thickness gauge before and after dipping inside PMMA solution. The difference of thickness of the probe after coating gives the measure of the coated film thickness. A large number of probes are coated with the film thickness between 5 μm to 12 μm. And the probes with uniform film thickness has been selected for experimentation.

The porosity in the film is developed due to the evaporation of chloroform in the drying process of film deposition. The final film quality and morphology depends on the solvent employed, state of substrate surface, deposition rates, type of ionic species and inert additives involved. The electrical, mechanical as well as structural features of polymeric films [22], [23] depends on the fabrication process. Figure 3 shows the Scanning Electron Microscope (SEM) image of the bare electrode surface before PMMA film coating. Figures 4 and 5 are the SEM images of the PMMA coated surface with coating thickness of 5 μm and 12 μm respectively, which have been obtained by dipping the probe inside 2.5% and 5% PMMA solution respectively. The dip-in time is 5-10 s. The thickness of the coating film can be varied by varying the dip-in time. From Figures 4 and 5, it can be observed that the coating film has a regular porous structure. The diameter of the circular pores of the coating surface decreases for larger coating thickness. Diameter of the smaller pore (12 μm coating thickness) is approximtely 5 μm and that of bigger pore (with coating thickness 5 μm) is

about 10 μm. That means, size of the micropore varies with the coating thickness, if the coating thickness is increased pore size decreases; and for about 50 μm coating thickness, the surface is nonporous and the probe behaves as a capacitance.

III. The CPA behaviour of the porous electrode

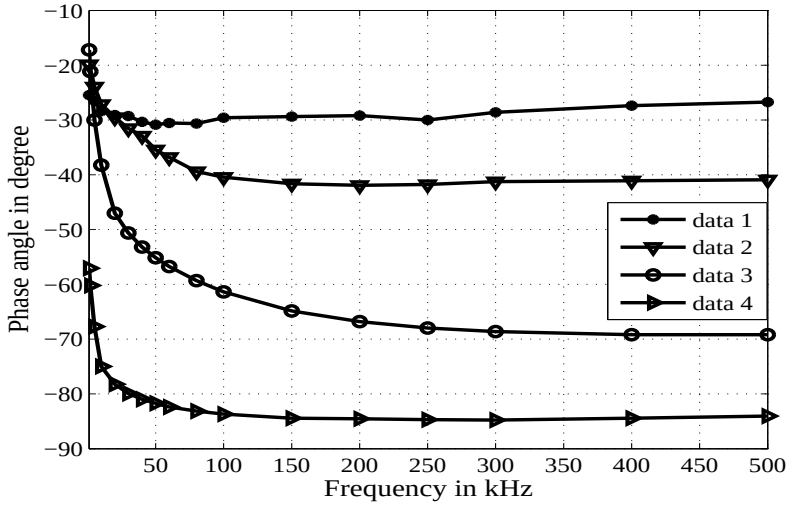

Figure 6. The CPA behaviour of four different CPE with different coating thickness. Data 1: 5 μm coating thickness, data 2: 12 μm coating thickness, data 3: 28 μm coating thickness, data 4: 47 μm coating thickness. The probe is dipped in tapwater.

It has been noticed that the constant phase angle(θ_{CPE}) is a function of the ionic property of the polarizable medium, the area of contact of the probe with the polarizable medium and the thickness of PMMA coating on the electrodes [24].

$$\theta_{CPE} = f(t, A, \sigma) \tag{2}$$

where, t is the thickness of the insulation on the electrode, A is the area of contact of the electrodes with the polarizing medium and σ is the ionic concentration of the polarizing medium. It can be observed from Figure 6 that the phase angle can be varied by a considerable amount by changing the thickness of the coating. The CPA behaviour of the two CPEs with two different porosity in different ionic media are shown in the Figure 7.

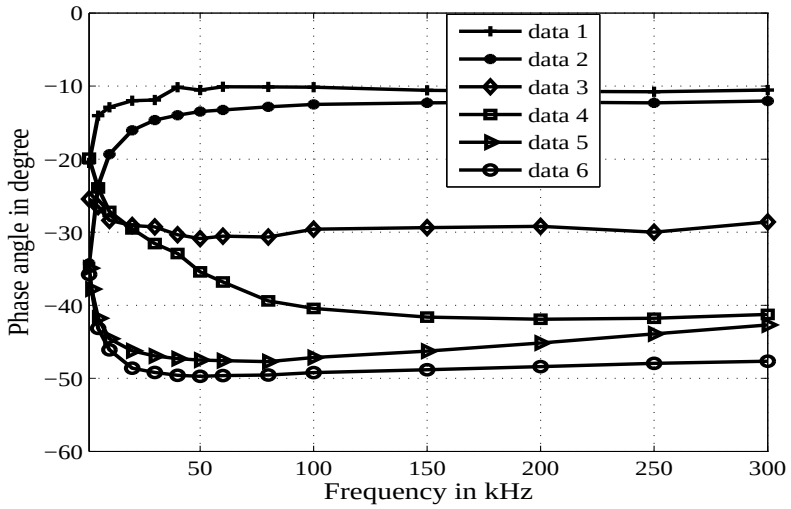

Figure 7. CPA behaviour obtained for two different porosity, data 1,2: 1M KCl, data 3,4: tap water(conductivity = 239μmho/cm), data 5,6: 9.2 pH. Data 1,data 3 and data 5 are for bigger pore (5 μm coating thickness); data 2, data 4 and data 6 are for smaller pore (12 μm coating thickness).

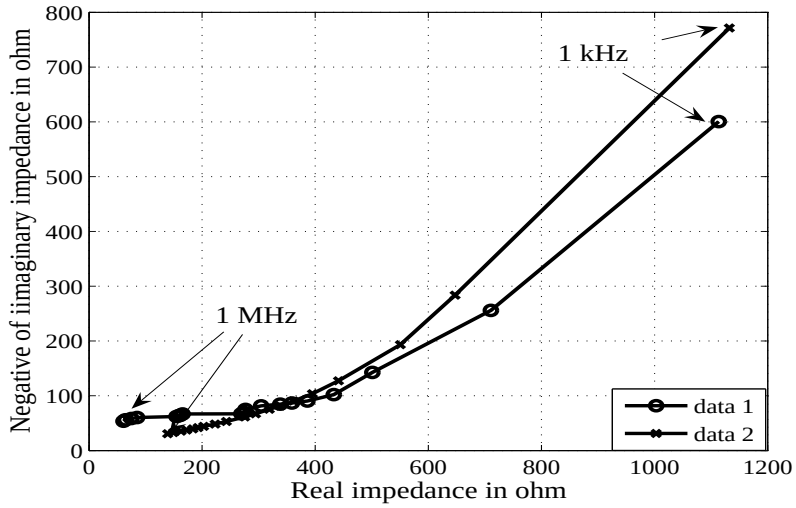

Figure 8. Real versus Imaginary impedance plot in 1M KCl, data 1: porous electrode with 5 μ coating thickness, data 2: porous electrode with 12 μm coating thickness.

IV. Complex impedance plots of porous electrodes

Researchers working in the field of electrochemistry have observed that diffusion of ions through a porous electrode gives rise to the CPA behaviour in the impedance spectra. Dif-

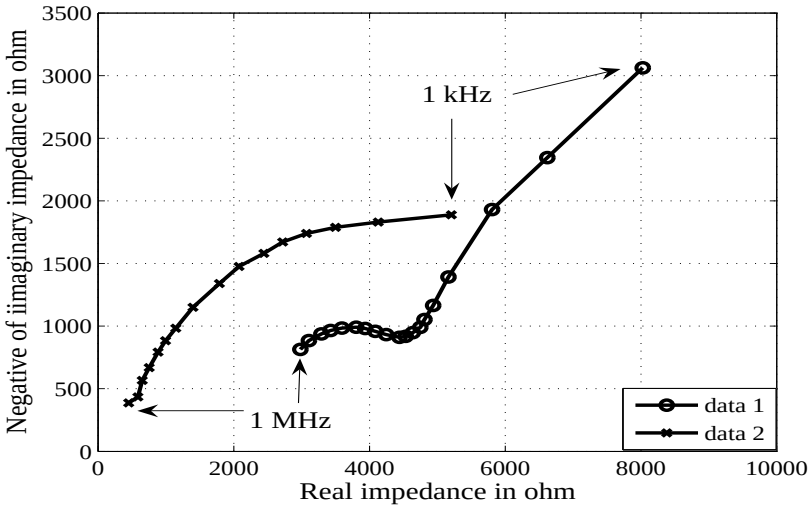

Figure 9. Real versus imaginary impedance plot in tap-water (conductivity = 239μmho/cm), data 1: porous electrode with 5 μm coating thickness, data 2: porous electrode with 12 μm coating thickness.

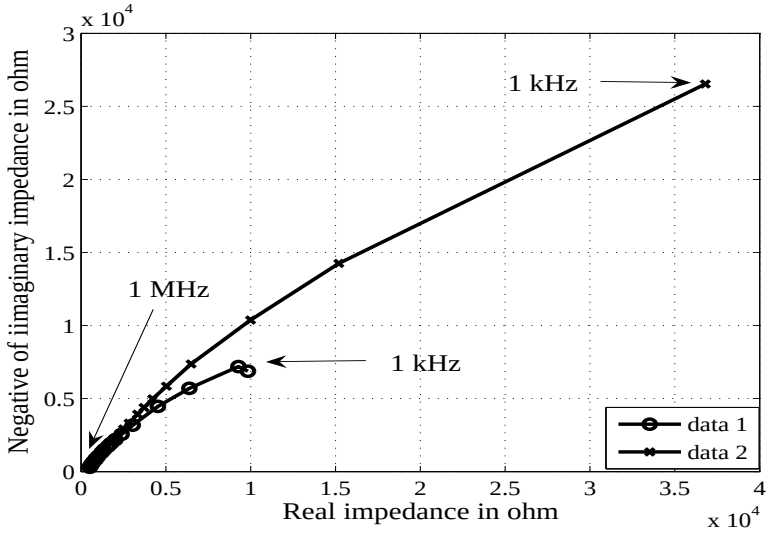

Figure 10. Real versus imaginary impedance plot in 9.2 pH solution, data 1: porous electrode with 5 μm coating thickness, data 2: porous electrode with 12 μm coating thickness.

ferent types of diffusion phenomenon, namely reflecting and adsorbing condition have been reported in the literature [5], [10], [11]. It is also of interest to study the diffusion phenomenon of the constructed CPE through EIS.

The complex impedance plots for the CPEs are shown in the Figures 8, 9 and 10. The

graphs are obtained from the real and imaginary impedances of the CPEs obtained with a precision LCR meter (explained in Section: I) in R, X mode. To perform the experiment the CPEs were dipped in the ionic medium one by one. For a particular measurement the area of contact of the probe with the ionic medium is kept constant. Figures 8, 9 and 10 show the complex impedance plot in 1M KCl solution, in tap water (with conductivity 230 μmho/cm) and in a standard alkaline solution (pH = 9.2), respectively.

V. CPE as a chemical sensor

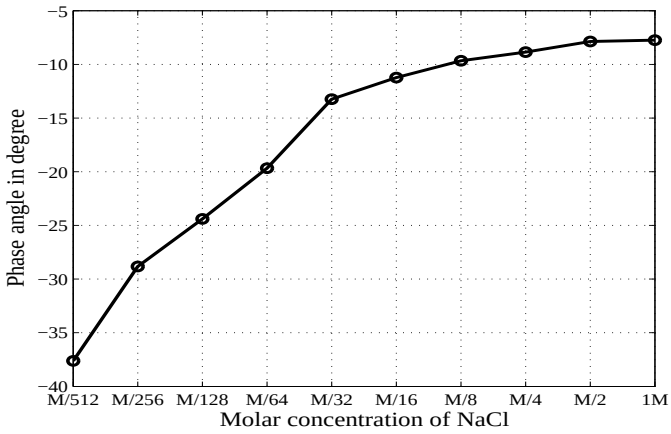

Figure 11. The CPA reading of the sensor at different concentration of NaCl solutions.The readings are taken at 100 kHz in the CPA zone.

The detection has two tasks. The first task is to measure the CPA (which is a function of the ionic property of the medium in which the probe is dipped in) and the second task involves the conversion of phase angle into electrical output. This means with the change of ionic environment, the phase angle is changed and a phase angle detector circuit gives the output in voltage. For the sensing purpose a fixed length (1 cm) of the probe (width 6 mm and coating thickness 12 μm) is dipped inside the medium so that the other parameters of the CPE remains constant.

To study the performance of the the sensor for chemical changes, different molar concentrations of NaCl, KCl, NH_4OH and Urea are considered. The concentration of the chemicals are varied from M/512 to 1M and phase angle is noted. It is worth to mention here that

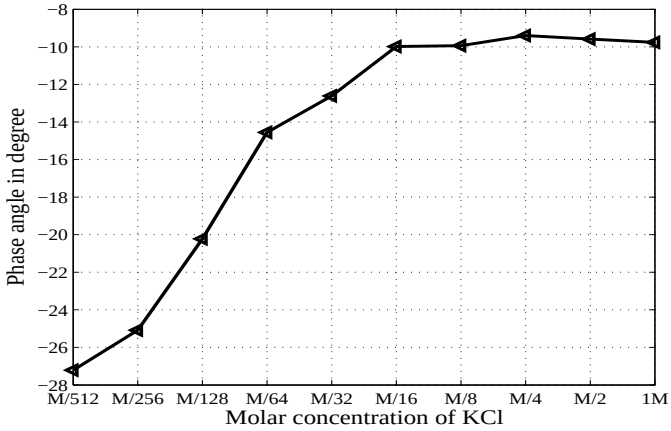

Figure 12. The CPA reading of the sensor at different concentration of KCl solutions.The readings are taken at 100 kHz in the CPA zone.

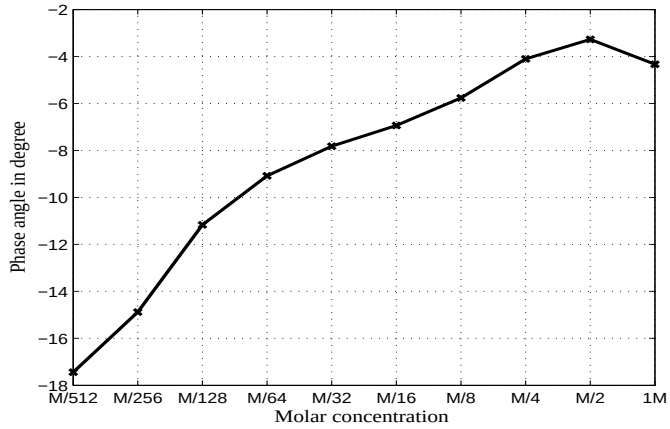

Figure 13. The CPA reading of the sensor at different concentration of NH_4OH solutions.The readings are taken at 100 kHz in the CPA zone.

the noted phase angle is constant for almost one decade of frequency (almost 50 kHz to 500 kHz), and the CPA is noted at a particular frequency (100 kHz) for all the measurements.The system takes about 30 secs to stabilize. In all the measurements, a fixed length (1 cm) of the probe is dipped inside the medium. The performance of the CPE at different molar solutions of NaCl, KCl, NH_4OH and Urea are shown in the Figures 11, 12, 13 and 14 respectively.

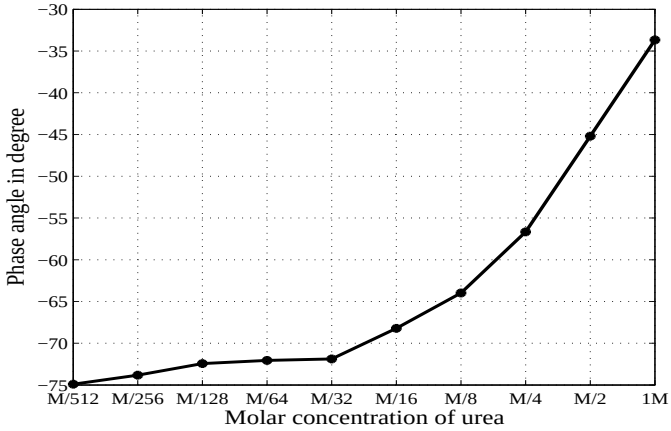

Figure 14. The CPA reading of the sensor at different concentration of Urea solutions.The readings are taken at 100 kHz in the CPA zone.

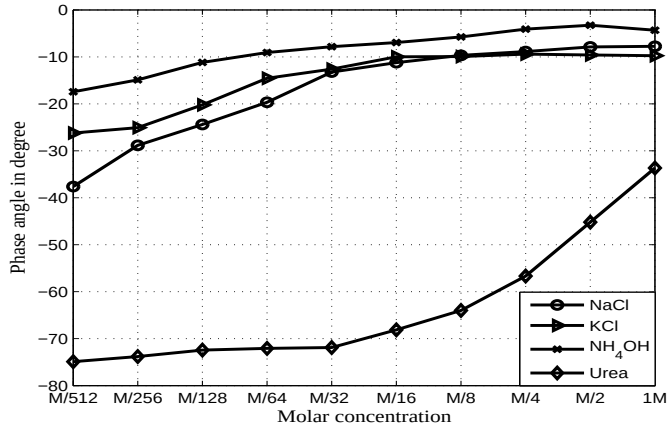

Figure 15. Comparison of responses between NaCl, KCl, NH_4OH and Urea solution at different molar concentration.

A. Phase angle detection

The phase detector circuit [25] is shown in the Figure 16. Sinusoidal excitation of 1 V peak at 100 kHz has been applied. One of the two amplifiers, at the first stage of the circuit, gets input directly from the signal generator and acts as a reference signal. The signal for the other amplifier comes through the CPE which is dipped inside the ionic medium. When the phase difference between the two inputs is zero the output voltage $v_0 = 0$; and when the phase difference is 90^o, it is maximum (half of the V_{DD} applied to the XOR gate chip).

In between, it gives an output voltage proportional to the phase difference between the two inputs which is a measure of the ionic concentration of the polarizing medium in which the CPE is dipped in. Figure 17a shows the variation of the phase angle of a microporous CPE at four standard solutions, and Figure 17b gives the corresponding electrical output.

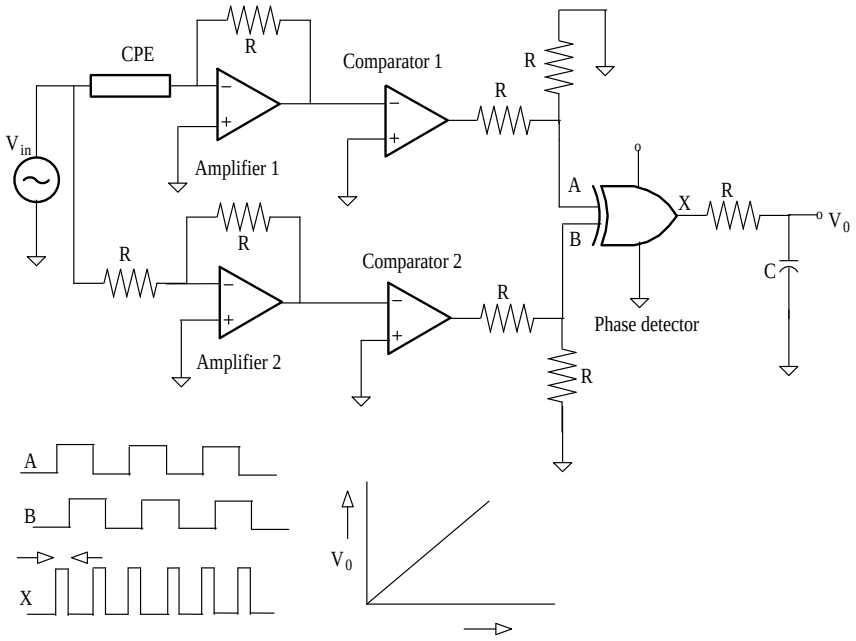

Figure 16. The phase angle detector circuit which gives the output in voltage with the phase angle input.

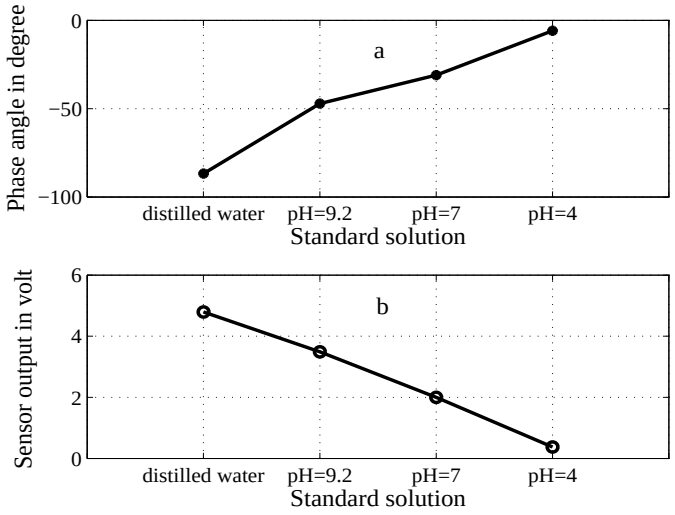

Figure 17. The performance of the CPE sensor in distilled water and three different pH solutions. (a) the value of the constant phase angle at different standard solutions, (b) The output voltage obtained from the detector circuit

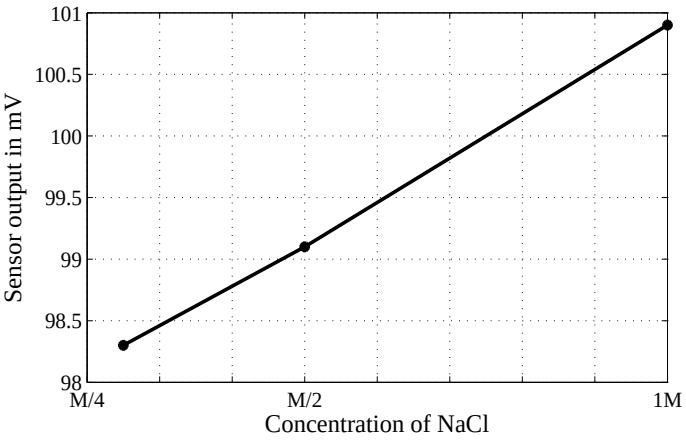

Figure 18. The performance of the CPE sensor in different concentrations of NaCl solutions

VI. Results and Discussion

The above results show that the CPA behaviour is due to the porous structure of the PMMA-film and the response is sensitive to the different chemical property of the medium in which the sensor is dipped in. From Figure 7 it can be observed that, for all the three polarizable media (1M KCl, tapwater, and standard alkaline solution(pH=9.2)), the magni-

tude of the CPA for the smaller porous electrode (5μm pore size) is greater than that of the bigger pore sized one (10 μm). It is also evident from the Figure 6 that, in tap water, the constant phase angle (in the frequency range of 50 kHz to 500 kHz) is about -30^0 for 5 μm pore diameter while for 10 μm pore diameter, the phase angle is about -40^0.

When we look into the complex impedance plots for these two probes - it can be observed that the responses resemble the different diffusion phenomenon reported by the researchers [10], [26]. The curves of Figure 8 are similar to the finite length diffusion curves with reflecting boundaries [27], where as in alkaline solution (pH=9.2) - the complex impedance plots (Figure 10) give adsorbing boundary of semi-infinite length diffusion [10]. This may be due to the fact that for the halide ions, the penetration depth through the porous surface is up to the metal electrode and from there it is reflected back. But in alkaline solution the penetration depth is less and we observe adsorbing condition of semi infinite diffusion [10], [28]. In tap water, ions of different species are present, and data 1 of Figure 9 shows a typical curve for the case involving two adsorbed species [27].

From the Figures 11, 12, 13 and 14, it can be observed that the sensor gives very consistence performance in the ionic media. For NaCl, KCl and NH_4OH solutions sensitivity is better at lower concentration. This may be due to the fact that after a certain level of ionic concentration, the diffusion through the porous surface becomes steady. This is also to be noted that at the same molar concentration, sensor gives different outputs for different chemicals as shown in the Figure 15. For example at M/512 molar concentration NaCl gives a phase angle of $-38°$, KCl gives phase angle around $-27°$ and NH_4OH gives phase angle around $-17°$ (Figure 15). The selectivity can be enhanced by careful design and standardization.

Urea is non ionic, so it does not change the ion concentration of distilled water. If Figure 14 and Figure 17a are compared, it can be seen that at lower concentration of Urea solution the phase angle is almost equal to the phase angle what we get for distilled water. But at higher concentration of Urea solution we can observe that the solution is ionised, this phenomenon is not very clear and needs further investigation. In Urea solution, the sensitivity is better at higher concentration. Here also at the same molar concentration the

phase angle for Urea is different than that of NaCl and KCl.

The phase detector circuit (Figure 16) is used to measure the voltage corresponding to the phase angle for four standard solutions. Figure 17a shows the variation of the phase angle of such a microporous CPE at four standard solutions (distilled water, standard pH solutions of 4, 7 and 9.2), and Figure 17b gives the corresponding electrical output. The phase angle for distilled water and for buffer solution of $pH = 7$ differs due to the fact that the positive ion concentration for both the solution are not same. Buffer solution of $pH = 7$ was prepared with the buffer tablet and may have positive ion present in it compared to the distilled water. The Figure 17 shows very consistence performance of the measurement in the four standard solutions. So, it can be said that the circuit can be used to convert the phase angle to voltage for NaCl (Figure 18), KCl, NH_4OH and Urea solutions.

VII. Conclusion

In this work, a thin porous film of PMMA is used to coat the electrodes of a rigid type probe. Due to the porous nature of the insulation coating it behaves as a CPE in polarizable medium for almost one decade of frequency. The phase angle versus frequency plots show that in the same ionic medium, constant phase angle of the CPE varies with the size of the pore.

From above results and discussions it is apparent that the proposed CPE sensor can be used for various chemical sensing. In pollution control, measurement of water contamination due to urea is important for fish culture as the fish is consumed as food. In many pathological diagnosis measurement of urea is involved [29] which can be performed with the proposed sensor. In food processing and biotechnology, measurement of ionic concentration of the medium is involved as the microbial growth changes the ionic property of the medium [21]. Hence, the constructed CPE may be an alternative to the many sensors presently used in these fields.

It is expected that the study will help to design a CPE sensor, though, advance studies are required to achieve the desired phase angle of the CPE. The proposition of electrical equivalent circuit may form an interesting research topic. Further studies are on in this

direction using Complex Nonlinear Least Squares [30] fitting of the EIS data.

Further,the PMMA-film on the electrode surface makes it bio-compatible, heat resistant, and rugged [31]. The major advantages are that the sensor does not contaminate the process under test and very easy to construct hence, cheap. The device is a single probe with two terminals and hence, can be easily connected to the electronic circuits.

References

[1] A. Ur, D. F. Brown, Impedance monitoring of bacterial activity, Journal of Medical Microbiology 8 (1975) 19–27.

[2] R. Gomej-Sjorberg, D. T. Morisette, R. Bashir, Impedance microbiology-on-a-chip: Microfluidic bioprocessor for rapid detection of bacterial metabolism, Journal of Microelectromechanical Systems 14 (4) (2005) 829–838.

[3] R. Gomej-Sjorberg, R. Bashir, A. Bhunia, Microscale electronic detection of bacterial metabolism, Sensors and Actuators B: Chemical 86 (2-3) (2002) 198–208.

[4] A. Andresscu, O. A. Sadik, Trends and challenges in biochemical sensors for clinical and environmental monitoring, Pure and Applied Chemistry 76 (2004) 861–878.

[5] J. R. Macdonald, Impedance Spectroscopy Emphasizing Solid Materials and Systems, John Wiley and sons, 1987.

[6] P. Zoltowski, On the electrical capacitance of interfaces exhibiting constant phase element behavior, Journal of Electroanalytical Chemistry 443 (1998) 149–154.

[7] M. Itagaki, A. Taya, K. Watanabe, K. Noda, Deviation of capacitive and inductive loops in the electrochemical impedance of a dissolving iron electrode, The Japan Society of Analytical Chemistry 18 (2002) 641–644.

[8] K. Biswas, S. Sen, P. K. Dutta, Realization of a constant phase element and its performance study in a differentiator circuit, IEEE Transactions of Circuits and Systems-II 53 (2006) 802–806.

[9] K. B. Oldham, Semintegral electroanalysis: Analog implementation, Analytical Chemistry 45 (1) (1973) 39 – 47.

[10] A. Lasia, Electrochemical Impedance Spectroscopy and its Applications, Kluwer Aca-

demic/Plenum Publishers, New York, 1999.

[11] J. Bisquert, G. Garcia-Belmonte, F. Fabregat-Santiago, N. S. Ferriols, P. Bogdanoff, E. C. Pereira, Doubling exponent models for the analysis of porous film electrodes by impedance: Relaxation of TiO_2 nanoporous in aqueous solution, Journal of Physical Chemistry 104 (2000) 2287–2298.

[12] S. C. D. Roy, On the realization of a constant-argument immitance or fractional operator, IEEE Transaction on Circuit Theory CT-14 (1967) 264–274.

[13] G. E. Carlson, C. A. Halijak, Approximation of fractional capacitors $(1/s)^{1/n}$ by a regular newton process, IEEE Transaction on Circuit Theory (1964) 210–213.

[14] A. Oustaloup, F. Levron, B. Mathieu, F. M. Nanot, Frequency-band complex noninteger differentiator: Characterization and synthesis, IEEE Transactions on Circuit and Systems 47 (1) (2000) 25–39.

[15] B. Mathieu, P. Melchior, A. Oustaloup, C. Ceryal, Fractional differentiation for edge detection, Signal Processing 83 (2003) 2421–2432.

[16] O. P. Agrawal, Application of fractional derivatives in thermal analysis of disk brakes, Nonlinear Dynamics 38 (1-4) (2004) 191–206.

[17] I. Podlubny, Fractional-order systems and $PI^{\lambda}D^{\mu}$ controllers, IEEE Transaction on Automatic Control 44 (1) (1999) 208–214.

[18] M. F. Silva, J. A. T. Machado, A. M. Lopes, Fractional order control of a hexapod robot, Nonlinear Dynamics 38 (1-4) (2004) 417–433.

[19] H. Zhao, J. Yu, A simple and efficient design of variable fractional delay FIR filters, IEEE Transactions on Circuit and Systems-II 53 (2) (2006) 157– 160.

[20] M. D. Ortigueira, A. Guimaraes, A fractional linear view of the fractional brownian motion, Nonlinear Dynamics 38 (1-4) (2004) 295–303.

[21] K. Biswas, S. Sen, P. K. Dutta, A constant phase element sensor for monitoring microbial growth, Sensors and Actuators B: Chemical 119 (2006) 186–191.

[22] G. Garcia-Belmonte, Effect of electrode morphology on the diffusion length of the doping process of electronically conducting polypyrole films, Electrochemistry Communication 5 (2003) 236–240.

[23] L. Thomas, Study and modelling of impedance characteristics of PMMA-coated electrode in polarizable medium, Master's thesis, Department of Electrical Engineering, Indian Institute of Technology, Kharagpur (May 2006).

[24] K. Biswas, Studies on design, development and performance analysis of capacitive type sensors, Ph.D. thesis, Indian Institute of Technology Kharagpur, India, Department of Electrical Engineering (February 2007).

[25] D. Wobschall, Circuit Design for Electronic Instrumentation, McGraw-Hill, USA, 1979.

[26] J. Bisquert, G. Garcia-Belmonte, P. Bueno, E. Longo, L. O. S. Bulhoes, Impedance of constant phase element CPE-blocked diffusion in film electrodes, Journal of Electroanalytical Chemistry 452 (1998) 229–234.

[27] J. Bisquert, A. Compte, Theory of electrochemical impedance of anamolous diffusion, Journal of Electroanalytical Chemistry 499 (2001) 112–120.

[28] J. Bisquert, Theory of the impedance of electron diffusion and recombination in a thin layer, Journal of Physical Chemistry 106 (2002) 325–333.

[29] D. G. Pijanowska, M. Dawgul, W. Torbicz, Comparison of urea determination in biological samples by enfets based on pH and pNH_4 detection, Sensors 3 (2003) 160–165.

[30] J. Ross Macdonald and Solarton Group Limited, LEVMW, version 8.07; August, 2005, Immittance, Inversion, and simulation Fitting Programs for Windows and MS-DOS.

[31] R.-H. Horng, P. Han, H.-Y. Chen, K.-W. Lin, T.-M. Tsai, J.-M. Zen, PMMA-based capillary electrophoresis electrochemical detection microchip fabrication, Journal of Micromechanics and Microengineering 15 (2005) 6–10.